RSC Advances

ROYAL SOCIETY OF CHEMISTRY

www.rsc.org/advances

Journal Name

ARTICLE

Improving the electrochemical properties of polyamide 6/polyaniline electrospun nanofibers by surface modification with ZnO nanoparticles

Received 00th January 20xx,
Accepted 00th January 20xx

DOI: 10.1039/x0xx00000x

www.rsc.org/

R. S. Andre,[a,b] A. Pavinatto,[a] L. A. Mercante,[a] Elaine C. Paris,[a,b] Luiz H. C. Mattoso[a,b] and Daniel S. Correa[a,b]*

Heterostructured nanomaterials have attracted increasing interest because of their novel and distinct optical and electrical properties, finding applications in devices and chemical sensors. Here we report a new electrochemical platform based on the modification of fluorine doped tin oxide (FTO) electrode with polyamide 6/polyaniline (PA6/PANI) electrospun nanofibers decorated with ZnO nanoparticles. The nanoparticles were synthesized by co-precipitation method, followed by hydrothermal treatment, which route was optimized in order to obtain particles of small average diameter (45 nm). Polymeric nanofibers were obtained by the electrospinning technique and further subjected to the ZnO modification by nanoparticle impregnation. SEM images confirmed the uniform distribution of ZnO nanoparticles adsorbed onto the nanofibers surface, which amount was estimated to be 4% w/w, according to thermal gravimetric analysis (TGA). According to the electrochemical characterization, an improvement in electron transfer kinetic and increase in electroactive area was observed for the ZnO-modified electrode. The modified electrode was employed for monitoring hydrazine, and yielded a detection limit of 0.35 µmol.L^{-1}. Our results indicate that the novel sensing platform based on the adsorption of ZnO nanoparticles onto the surface of electrospun nanofibers can be potentially harnessed for electrochemical sensors and biosensors applications.

1. Introduction

Organic-inorganic hybrid materials have attracted increasing attention due to their potential application in different areas, including optics and electronics.[1,2] In most cases, the combination of organic and inorganic materials can yield a high-performance hybrid material with synergistic behaviors or complementary properties between the polymer and the inorganic component.[3-7] In fact, the combination of polymers and inorganic nanoparticles displays advantageous electrical, optical and mechanical properties, finding applications in opto-electronic devices and also as catalyst, which depends directly on the choice of the organic and inorganic component.[8,9]

A huge variety of polymeric structures could be used for this propose and 1D nanomaterials have been intensively investigated due to their unique properties.[10] Various techniques have been developed to fabricate 1D nanostructures, including the electrospinning technique, which is a versatile and low-cost method that can produce large specific surface area nanofibers.[11,12] This relatively huge surface area can potentially provide ultra-high sensitivity and fast response time for sensing applications.[13-17] In particular, electrospun nanofibers containing conductive polymer such as polyaniline (PANI) have attracted even more interest because of their high conductivity and potential applications in electrochemical devices.[18] In order to improve their properties and to construct multifunctional hybrid nanostructures, more recently considerable efforts have been directed towards attaching metallic and oxide NPs onto electrospun nanofibers.[19,20]

Zinc oxide (ZnO) is a versatile n-type metal oxide semiconductor with a wide band gap (3.36-3.39 eV) at room temperature, and present appealing features such as biocompatibility, nontoxicity and inexpensiveness.[21] It has been extensively used in the fabrication of electronic and optical devices, heterogeneous catalysis and gas sensing.[22] Furthermore, ZnO can be employed to facilitate the charge transfer and enhance the electrochemical activity.[23]Therefore, functionalizing electrospun nanofibers with NPs in order to combine the conductivity of the polymeric phase (PANI) and the high surface area of the nanofibers with the unique

[a] National Laboratory for Nanotechnology in Agribusiness (LNNA), Embrapa Instrumentation, 13560-970, São Carlos, SP, Brazil.
[b] Center for Exact Sciences and Technology, Department of Chemistry, Federal University of São Carlos (UFSCar), 13565-905, São Carlos, SP, Brazil.
Corresponding author E-mail: daniel.correa@embrapa.br
DOI: 10.1039/x0xx00000x

properties of ZnO NPs, can become an important strategy for the development of new electrochemical platforms.

In this context, herein we report an effective route to obtain fluorine doped tin oxide (FTO) electrode modified with polyamide 6/polyaniline (PA6/PANI) electrospun nanofibers decorated with ZnO nanoparticles. The hybrid nanomaterial combines the semiconductor properties of ZnO nanoparticles, synthesized by hydrothermal method, the conductive properties of PANI and the mechanical properties of PA6 in the same platform. X-Ray diffraction confirmed the ZnO formation, while the size and shape of nanoparticles were analyzed by field emission scanning electron microscopy (FEG-SEM). The efficient ZnO impregnation on the PA6/PANI nanofibers surface was confirmed by scanning electron microscopy (SEM). Electrochemical measurements were carried out to confirm the improvement in charge transfer efficiency of the PA6/PANI- ZnO modified electrode. In order to confirm the potential of this novel platform for sensing applications, we used hydrazine, a carcinogenic contaminant found in trace amounts in the environment,[24] as a model for the electrochemical measurements. The hydrazine sensor showed a linear range from 0.5 to 5000 μmol.L^{-1} and a detection limit of 0.35 μM.

2. Experimental

2.1 Materials

Polyamide 6 (PA6, Mw = 20 000 g.mol^{-1}), polyaniline (PANI, Mw = 20 000 g.mol^{-1}), zinc nitrate hexahydrate, Polyethylene glycol (PEG400, Mw = 380-420 g.mol^{-1}; PEG 4000, Mw = 3600-4400 g.mol^{-1}; PEG8000, Mw = 7000-9000 g.mol^{-1}) were all purchased from Sigma-Aldrich. Potassium hydroxide and formic acid were purchased from Synth Chemical (São Paulo, Brazil).Thedispersing agent, Liosperse 511, was purchased from Miracema-Nuodex (Campinas, Brazil).

2.2 Synthesis of ZnO nanoparticles

ZnO synthesis was carried out by coprecipitation method followed by hydrothermal treatment at 150 °C for 1 hour.[25]Initially, zinc nitrate and potassium hydroxide were separately dissolved in deionized water (0.05 mol.L^{-1} and 2 mol.L^{-1}, respectively) under vigorously stirring. PEG solution (0.1mol.L^{-1}) was added into the zinc nitrate solution for each synthesis and stirred for 30 minutes. Subsequently, potassium hydroxide solution was slowly added until pH 14 was reached. The suspension containing the white solid precipitate was then submitted to the hydrothermal treatment. The suspension was heated up at a rate of 10 °C/min under constant pressure (approximately 3.0 bar) until 150 °C and maintained at this temperature for 1 hour. Finally, the white solid was washed with deionized water several times until the pH became neutral and then dried in an oven.

2.3 Electrospinning of PA6 and PA6/PANI nanofibers.

PA6/PANI solution was prepared by dissolving 20% (w/v) PA6 and 1% (w/w) PANI in formic acid and stirred for 5h at room temperature. The electrospun nanofibers were obtained by using an electrospinning apparatus at a feed rate of 0.01 mL.$h^{-1}$and an electric voltage of 25 kV. A working distance of 10 cm was kept between the syringe and the metallic collector. The inner diameter of the steel needle was 1.2 mm. The produced nanofibers were directly electrospun onto fluorine doped tin oxide (FTO) glass substrates to obtain the modified electrodes. The substrates were attached to the collector at the same position in all experiments with an optimal collection time of 10 min. Control of the experimental conditions was crucial to ensure reproducibility because both the diameter and length of nanofibers depend on the collecting time and other experimental parameters.

2.4 Adsorption of ZnO nanoparticles onto the electrospun nanofibers

ZnO nanoparticles (1 mg.mL^{-1}) were dispersed in distilled water containing 0.5% (w/w) of Liosperse 511. Ultrasonication at 20 kHz for 5 minwas then applied for the nanoparticles dispersion. After breaking up the dispersion, the electrospun nanofibers were immersed into the ZnO solution, rinsed with distilled water and dried under ambient conditions. Three different adsorption times were tested (12, 24 and 48 h) in order to determine the best electrochemical response.

2.5Physico-chemical Characterization

As-prepared samples of ZnO nanostructures were characterized by X-ray diffraction (XRD) using a Shimadzu, XRD-6000 diffractometer at 30 kV and 30 mA with Cu Kα radiation. Morphology and size characterizations were performed by field emission gun scanning electron microscopy (FEG-SEM) (JEOL, JSM 6510). The morphology of the fibers was evaluated using a scanning electron microscope (SEM, JEOL 6510) operating at 10 kV, and the fiber diameter was estimated by using an image analysis software (Image J, National Institutes of Health, USA). In each experiment, the average fiber diameter and distribution were determined by measuring 100 random fibers using representative micrographs. To estimate the amount of ZnO nanoparticles adsorbed onto the nanofiber surface, thermal gravimetric analysis (TGA) was performed using a thermogravimetricanalyzer (Q500 TA Instruments) under nitrogen atmosphere, at a flow rate of 20 ml.min^{-1}. Samples in platinum pans were scanned from room temperature to 1000°C at a heating rate of 10°C.min^{-1}.

2.6 Electrochemical Measurements

Electrochemical experiments were carried out using a PGSTAT30 Autolab electrochemical system (Metrohm). The nanofibers-modified-FTO electrodes were used as working electrodes. A Pt foil and Ag/AgCl (3 mol.L^{-1}KCl) electrodes

served as the counter and reference electrodes, respectively. Electrochemical impedance spectroscopy (EIS) measurements were carried using a 0.05 mol L^{-1} $[Fe(CN)_6]^{3-/4-}$ containing 0.1 mol.L^{-1}KCl at a potential of 0.3 V over the frequency range from 0.1 Hz to 100 kHz and with an amplitude of 10 mV. The performance of the sensing platform for hydrazine detection was evaluated by chronoamperometry using a potential of 0.8V.

3. Results and Discussion

3.1 Characterization of ZnO nanoparticles

Different molar weight PEGs were employed to optimize ZnO synthesis in order to obtain nanoparticles with suitable shape and size for impregnation onto the polymeric electrospun nanofibers. The long-range order of ZnO samples was determined by X-rays diffraction. Figure 1 shows XRD patterns of ZnO synthetized using (a) PEG 8000, (b) PEG 4000 and (c) PEG 400. All samples present the same diffraction peaks, which are attributed to polycrystalline ZnO. The pattern is typical of the ordered hexagonal wurtzite phase according to JCPDS Card N° 36-1451. Diffraction peaks related to secondary phases were not found, indicating that ZnO without impurities was successfully obtained for the three different molar weight PEGs tested.

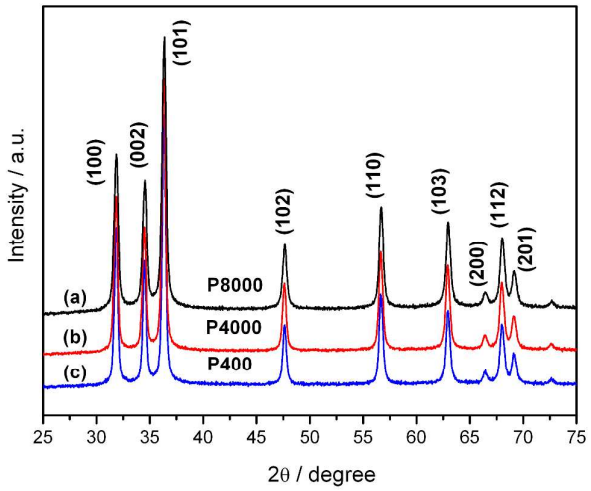

Figure 1.XRD patterns of ZnO synthetized with (a) PEG 8000, (b) PEG 4000 and (c) PEG 400.

As the desired phase was successfully obtained for all tested samples, they were analyzed by FEG-SEM to characterize the shape and size of the ZnO nanoparticles obtained. Surfactants have been employed to control the shape and size of nanostructures, once features such as hydrophobic chains, headgroups, impurity ions and concentration of surfactants exert direct effects on the nanoparticles properties. [26-28]

Using PEGs with high molecular weight (PEG8000 and PEG4000), agglomerated nanoparticles with a nearly spherical morphology and polydisperse nature were obtained (see Fig. 2 (a) and (b)). In hydrothermal conditions, the solubility of amorphous particles is significantly increased and crystallization can occur concurrently with redissolving and reprecipitation processes.[29,30] After the nucleation process, the increased particle solubility could result in growth of an individual nanostructure aggregation and/or coarsening.[25,31,32] PEG8000 and PEG 4000 were not very efficient as surfactants, yielding shapeless and large grain originated from random aggregation process between small particles. Thus, our results indicate that the use of PEG surfactant with longer hydrophobic chains leads to nanoparticles with larger sizes.[33] On the other hand, PEG 400, a hydrophobic surfactant with shorter molecular chain, yielded nanoparticles (see Fig. 2c) of low dispersion with homogeneous distribution and smaller size (44 nm), adjusted by lognormal fit, as shown in histogram of Figure 2d, configuring the best-optimized process and the choice for the subsequent studies.

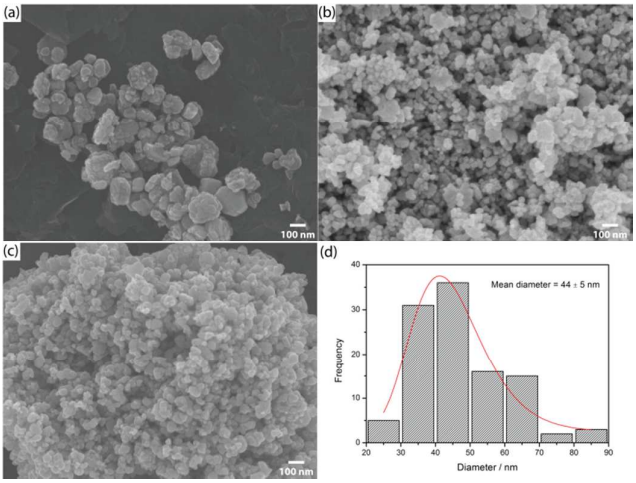

Figure 2.FEG-SEM images of ZnO synthetized with (a) PEG 8000, (b) PEG 4000 e (c) PEG 400. (d) Histogram of size distribution of ZnO nanoparticles synthetized with PEG 400.

3.2 Characterization of PA6/PANI nanofibers

To obtain uniform PA6/PANI electrospun nanofibers, the electrospinning parameters were optimized through variation of the flow rate, applied voltage, polymers concentration, and collection distance. Under the improved experimental parameters, smooth and uniform bead-free nanofibers were obtained with a mean diameter of 78 ± 1 nm, as shown in Figure 3a.

In order to improve the electrochemical properties of the fabricated nanofibers, a further step was taken aiming at functionalizing them with ZnO nanoparticles. ZnO-containing electrospun polymer nanofibers (PA6/PANI_ZnO) could exhibit a huge variety of potential applications, as the composite fibrous mats show flexibility, are freestanding and display

hybrid properties determined by the polymer and NPs.[34] In this way, the surface of PA6/PANI nanofibers was efficiently modified with ZnO nanoparticles, as confirmed by the FEG-SEM image in Figure 3b. The typical image of the PA6/PANI_ZnO nanofibers indicates that the coating on the nanofibers surface appears to be uniform. Moreover, the adsorption was strong since the nanoparticles remained on the nanofibers surface even after a washing process, consisting of repeated submersion in water, was applied for several times. This suggests that the ZnO NPs are not simply lying on the nanofiber surface, but instead, they are attached to the PA6/PANI nanofibers via H-bonding and electrostatic interaction.

The adsorption of ZnO on nanofibers can occur through an interaction between the negatively charged COO- groups from the surfactant Liosperse (based on ammonium polyacrylate) present on the ZnO surface and the positively charged sites from PANI present on the nanofibers.[35] H-bonding may take place between the carboxylic groups (-COOH) of the surfactant and imine nitrogens and/or amine nitrogens of PANI and amide groups from PA6.[36] The Energy Dispersive Spectrometer (EDS) of the modified PA6/PANI nanofibers was carried out in order to prove the presence of ZnO on the nanofibers surface (inset Figure 3b).

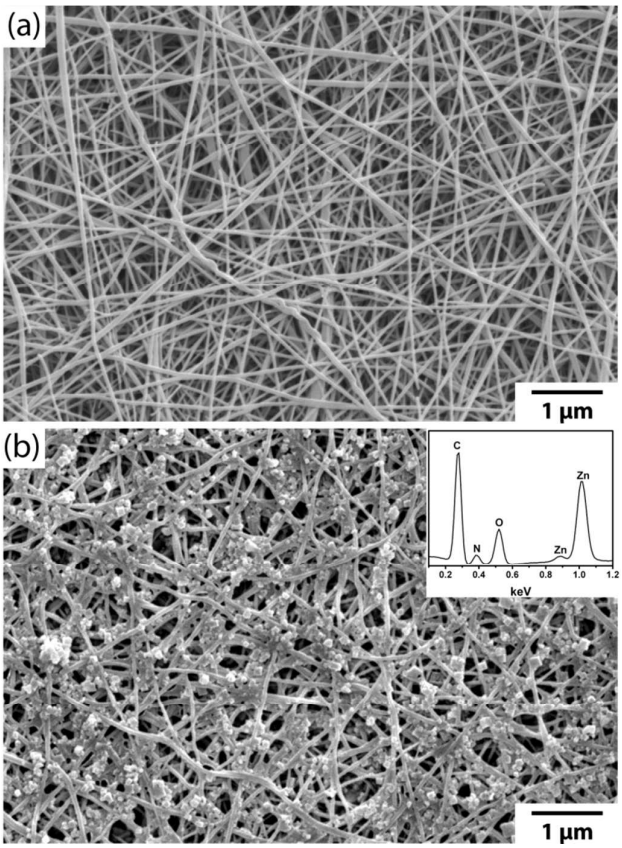

Figure 3.SEM images of (a) PA6/PANI and (b) PA6/PANI_ZnO nanofibers. The inset in panel (b) shows the EDS spectra of PA6/PANI_ZnO.

The amount of ZnO nanoparticles adsorbed onto the nanofiber surface was determined by thermal gravimetric analysis (TGA). Figure 4 shows TGA curves of ZnO nanoparticles (solid line), PA6/PANI (dashed line) and PA6/PANI_ZnO (dotted line) nanofibers. Pure ZnO nanoparticles start to degrade only at 860°C due its high temperature stability. Both PA6/PANI and PA6/PANI_ZnO exhibit a substantial weight loss, starting at 380°C and extending up to 470°C, resulting in the complete polymer decomposition. Based on the TGA curve for PA6/PANI_ZnO nanofibers is possible to estimate that the mass loading of nanoparticles on the nanofibers surface is around 4 wt.%.

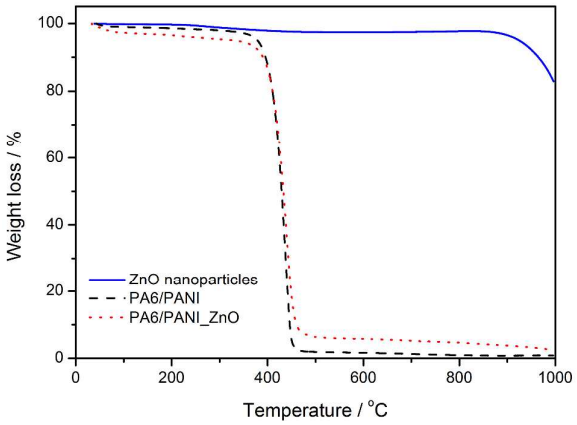

Figure 4.TGA curves of ZnO nanoparticles (solid line), PA6/PANI nanofibers (dashed line) and PA6/PANI_ZnO nanofibers (dotted line).

3.3 Electrochemical Measurements

ZnO is a metal oxide semiconductor with appealing electrical and optical properties, finding applications in and photovoltaic devices, gas sensing and electrochemical biosensor.[22,37,38] As demonstrated by microscopy results, ZnO nanoparticles were successfully adsorbed on the PA6/PANI electrospun nanofibers surface, which suggests a novel and potential platform for sensing application. In order to verify the ZnO influence on the conducting properties of PA6/PANI nanofibers, electrochemical measurements were carried out.

Figure 5 shows the (a) Nyquist plots for PA6/PANI_ZnO obtained with different ZnO adsorption times, (b) Nyquistplots and (c) cyclicvoltammogramsfor FTO, PA6/PANI and PA6/PANI_ZnO electrodes measured in the presence of 5 mmolL^{-1} $[Fe(CN)_6]^{3-/4-}$ in a 0.1 molL^{-1}KCl solution at a potential of 0.3 V. The Nyquist plots obtained for PA6/PANI_ZnO modified nanofibers obtained using different ZnO adsorption times (12, 24 and 48 hours) were interpreted using a Randle´s equivalent circuit, shown in inset (i) of Fig. 5 (b). The Nyquist plot of EIS includes a linear region at low frequency related to the diffusion-limited process, while the semicircular region at high frequencies is related to the electron-transfer-limited process, where the diameter corresponds to the charge (electron) transfer resistance

(R_{ct}).[23]The highest R_{ct} value (41 Ω) was found to ZnO-modified PA6/PANI nanofibers electrode immersed for 12 hours in ZnO solution, while a similar R_{ct} value of nearly 15 Ω was found for electrodes immersed for 24 and 48 hours, respectively. The results suggest that the adsorption of ZnO nanoparticles on the PA6/PANI nanofibers tends to reach the saturation in 24 hours, and therefore this was the time chosen for the electrode immersion.

Figure 5b presents Nyquist diagrams for FTO, PA6/PANI and PA6/PANI_ZnO, whose data were again interpreted using the Randle´s equivalent circuit (see inset (i)-Fig. 5 (b)). The Nyquist diagrams yielded aR_{ct} value of 15 Ω for the PA6/PANI_ZnO electrode, while values of 36 Ω and 39 Ω were found for the bare FTO and PA6/PANI electrodes, respectively. The lowest R_{ct} value for the modified PA6/PANI electrode with ZnO nanoparticles was obtained as a consequence of a faster electron transfer process. Such improvement in charge transfer process occurs thanks to the conducting properties of ZnO nanoparticles.

The voltammograms, displayed in Figure 5c, show a quasi-reversible one-electron redox behavior, where Ipa/Ipc ~1, for all electrodes, with increase in anodic peak current from 479 µA to 585 µA and cathodic peak current from 432 µA to 578 µA, comparing the values for bare FTO and PA6/PANI_ZnO electrode, respectively. Furthermore, the reduction in peak separation (ΔEp) from 190 mV for bare FTO electrode to 180 mV for PA6/PANI_ZnO modified electrode confirms the faster electron transfer kinetic that is promoted by ZnO nanoparticles. On the other hand, Ipa, Ipc and ΔEp values for the PA6/PANI electrode voltammograms was found to be 447 µA, 432 µA and 190 mV, respectively. Furthermore, the electroactive area of the electrodes, i.e. the real area transferring charge to the redox probes, was estimated according to the Randles-Sevcik equation[39,40] using the cathodic peak current obtained from the voltammograms. The electroactive areas were calculated to be 0.41, 0.37 and 0.49 cm^2 for FTO, PA6/PANI and PA6/PANI_ZnO electrodes, respectively. The voltamogramms show that the PA6/PANI_ZnO modified nanofiber displayed an increase in the electroative area, which helps to enhance the electrochemical performance of the electrode. Therefore, both EIS and voltamogramms results suggest that modifying electrodes with ZnO nanoparticles/polymer nanofibers is a suitable strategy for improving charge-transfer process aiming at chemical sensing applications.

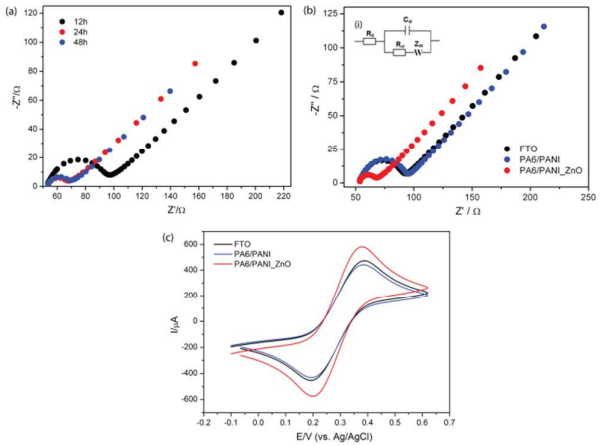

Figure 5. (a) EIS of PA6/PANI_ZnO electrode obtained with different ZnO adsorption times (b) EIS and (c) CVs of bare FTO, PA6/PANI and PA6/PANI_ZnO electrodes in 5 $mmolL^{-1}$ $[Fe(CN)6]^{-3/-4}$ solution with 0.1 mol L^{-1}KCl. The inset in panel b (i) shows the Randle's equivalent circuit model for the electrochemical data.

3.4 Electrochemical Detection of Hydrazine (N_2H_4)

In order to prove the potential application of the novel sensing platform, chronoamperometic measurements were employed for hydrazine (Hy) detection. Figure 6 shows amperometric response experiments using PA6/PANI_ZnO electrode with successive changes of Hy concentration. The calibration curve was constructed with concentrations ranging from 0.5 to 20000 µmol.L^{-1}, and show a linear range following the equation: I (µA) = - 0.870 [Hy](µmol.L^{-1}) + 0.027 (R^2= 0.994), corresponding to a concentration range from 0.5 to 5000 µmol.L^{-1} (inset). The limit of detection was estimated to be 0.35 µmol.L^{-1}, based on a signal to noise ratio of 3 (S/N = 3).

The reproducibility of the PA6/PANI_ZnO electrode was tested by performing repeated experiments with solutions containing 50 µmol.L^{-1} of Hy. Good reproducibility was reached for five successive measurements and the relative standard deviation (RSD) was calculated to be 3.5% for a given electrode, while it was found to be 5.5% when three identical electrodes were employed.

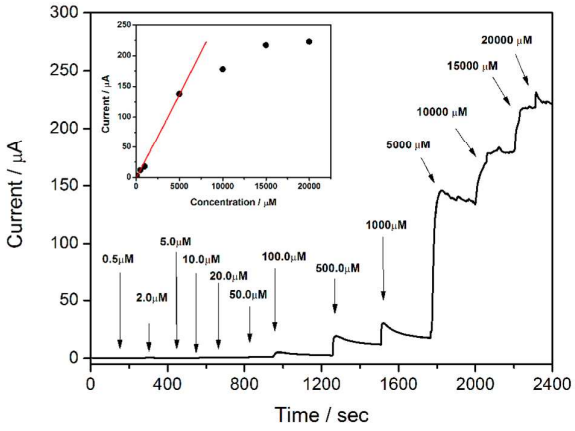

Figure 6. Amperometric current response of PA6/PANI_ZnO electrode in 0.01 mol.L^{-1} PBS (pH 7.5) for concentration range 0.5 to 20000 µmol.L^{-1} of Hy. The inset presents the linear relationship between current response and Hy concentrations.

The selectivity of PA6/PANI_ZnO electrode for Hy detection was verified by chronoamperometric technique using interfering compounds. The measurements were carried out using 20-fold excess of glucose and 25-fold excess of $CaCl_2$, $ZnO(NO_3)_2$ and $Cu(NO_3)_2$ in 100 µmol.L^{-1} of Hy solution in 0.01 molL^{-1} PBS (pH 7.5), which are considered potential interfering compounds for hydrazine detection.[41] The sensing platform proved to be selective for Hy detection, as displayed in Figure 7, with no significant interference in current response from the compounds.

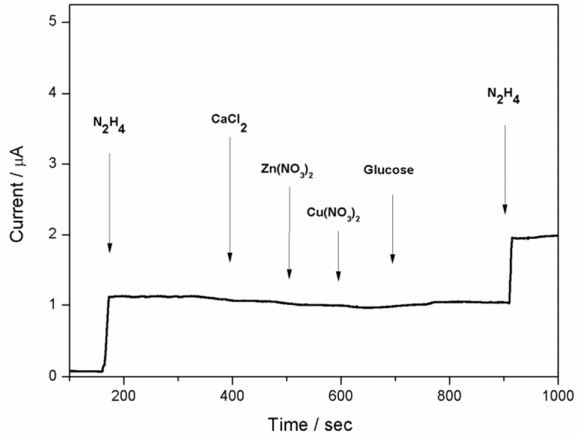

Figure 7. Selectivity amperometric current response of the PA6/PANI_ZnO sensor for Hy (N_2H_4) mixed with interferents in 0.01 mol.L^{-1} PBS (pH 7,5).

Furthermore, the PA6/PANI_ZnO electrode presented a Hy limit of detection and linear range of detection compatible to other sensing platforms (based on electrode modification) recently reported in the literature (Table 1). Our results show that the as-prepared platform is suitable for Hy detection even in the presence of distinct interferents, displaying good specificity and low limit of detection, which prompts it as a promising platform for sensor and biosensor design.

Table 1. Comparison of Linear range and Detection limit between hydrazine sensors based in similar ZnO structures.

Electrode Modification	Linear Range (µmol.L -1)	LOD (µmol.L^{-1})	Reference
ZnO Nanoparticles	0.5 - 5000	0.35	This work
ZnO NanoparticlesII	-----	0.147	42
ZnOMicro/nanoarc hiteture	0.8 - 200	0.25	43
ZnO NanoFilm	0.5 - 14200	0.5	44
ZnO-RGO	1 - 33500	0.8	41

4. Conclusion

A novel electrochemical platform was successfully fabricated by modifying FTO electrodes with PA6/PANI electrospun nanofibers and further decorating them with ZnO nanoparticles. Our results indicated that the ZnO nanoparticles remained strongly attached to the PA6/PANI nanofibers surface via H-bonding and electrostatic interaction. Electrochemical measurements revealed improvement in electron transfer kinetic for the ZnO-modified electrode, yielding the lowest Rct value (15 Ω) for the PA6/PANI_ZnO electrode when compared to bare FTO (36 Ω) and PA6/PANI electrodes (39 Ω), which is beneficial for electrochemical application. Additional experiments revealed that the novel platform is suitable for monitoring hydrazine in the presence of interfering compounds with a detection limit of 0.35µmol.L^{-1}. Ultimately, our results indicate that the ZnO decoration of PA6/PANI nanofibers provides a promising platform for designing electrochemical sensors and biosensors.

Acknowledgements

The authors thank the financial support from CNPq (141894/2013-0), FAPESP (Grant numbers: 2014/16789-5, 2012/23880-3 and 2013/26712-7), CAPES, MCTI-SisNano and EMBRAPA from Brazil.

References

1 L. Nicole, C. Laberty-Robert, L. Rozes, C. Sanchez, Nanoscale, 2014, **6**, 6267.
2 K. G. Sharp, *Adv. Mater.*, 1998, **10**, 1243.
3 A. Convertino, G. Leo, M. Striccoli, G. Di Marco, M. L.Curri, *Polymer*, 2008, **49**, 5526.
4 M. Scocioreanu, M. Baibarac, I. Baltog, I. Pasuk, T. Velula, *J. Solid State Chem.*, 2012, **186**, 217.
5 E. Gianotti, U. Diaz, S. Coluccia, A. Corma, *Phys. Chem. Chem. Phys.*, 2011, **13**, 11702.
6 E. Kim, Y. Lee, J. Bang, K. Kim, S. Choe, *Mater. Chem. Phys.*, 2012, **134**, 814.
7 A. Manzoli, F. M. Shimizu, L. A. Mercante, E. C. Paris, O. N. Oliveira Jr, D. S. Correa, L. H. C. Mattoso, *Phys. Chem. Chem. Phys.*, 2014, **16**, 24275.
8 C. Sanchez, P. Belleville, M. Popall, L. Nicole, Chem. Soc. Rev., 2011, 40, 696-753.
9 B. T. Raut, P. R. Godse, S. G. Pawar, M. A. Chougule, D. K. Bandgar, S. Sen, V. B. Patil, *J. Phys. Chem. Solids*, 2013, **74**, 236.
10 X. Lu, C. Wang, Y. Wei, Small, 2009, 5, 2349-2370.
11 J. Wu, N. Wang, Y. Zhao, L. Jiang, *J. Mater. Chem. A*, 2013, **1**, 7290.

12 R. Sahay, P. S. Kumar, R. Sridhar, J. Sundaramurthy, J. Venugopal, S. G. Mhaisalkar, S. Ramakrishna, J. Mater. Chem., 2012, **22**, 12953.

13 B. Ding, M. Wang, J. Yu, G. Sun, *Sensors*, 2009, **9**, 1609.

14 L. A. Mercante, A. Pavinatto, L. E. O. Iwaki, V. P. Scagion, V. Zucolotto, O. N. Oliveira Jr., L. H. C. Mattoso, D. S. Correa, *ACS Appl. Mater. Interfaces*, 2015, **7**, 4784.

15 A. P. Roque, L. A. Mercante, V. P. Scagion, J. E. Oliveira, L. H. C. Mattoso, L. De Boni, C. R. Mendonca, D. S. Correa, *J. Polym. Sci. Pol. Phys.*, 2014, **52**, 1388.

16 J. E. Oliveira, V. P. Scagion, V. Grassi, D. S. Correa, L. H. C. Mattoso, *Sens. Actuators B*, 2012, **171**, 249.

17 Y. Lv, Y. Zhang, Y. Du, J. Xu, J. Wang, *Sensors*, 2013, **13**, 15758.

18 L. T. H. Nguyen, S. Chen, N. K. Elumalai, M. P. Prabhakaran, Y. Zong, C. Vijila, S. I. Allakhverdiev, S. Ramakrishna, Macromol.*Mater. Eng.*, 2013, **298**, 822.

19 J. Wu, F. Yin, *Sens. Actuators B*, 2013, **185**, 651.

20 Y. Huang, Y. -E. Miao, S. Ji, W. W. Tjiu, T. Liu, *ACS Appl. Mater. Interfaces*, 2014, **6**, 12449.

21 S. Jagtap, K. R. Priolkar, *Sens. ActuatorsB*, 2013, **183**, 411.

22 S. Park, S. An, H. Ko, C. Jin, C. Lee, *ACS Appl. Mater. Interfaces*, 2012, **4**, 3650.

23 L. Fang, K. Huang, B. Zhang, B. Liu, Y. Liu, Q. Zhang, *RSC Adv.*, 2014, **4**, 48986.

24 U.S. Department of Health and Human Service, Hazardous Substances Data Bank (HDBS, online database), National Toxicology Information Program, National Library of Medicine, Bethesda, MD, 1993.

25 S. Baruah, J. Dutta, *Sci. Technol. Adv. Mater.*, 2009, **10**, 013001-18.

26 J. Xiao, L. Qi, *Nanoscale*, 2011, **3**, 1383.

27 W. Guo, T. Liu, H. Zhang, R. Sun, Y. Chen, W. Zeng, Z. Wang, *Sens. Actuators B*, 2012, **166-167**, 492.

28 Z. Li, Y. Xiong, Y. Xie, *Inorg. Chem.*, 2003, **42**, 8105.

29 S. A. Norris, S. J. Watson, *ActaMater.*, 2007, **55**, 6444.

30 M. Lin, Z. Y. Fu, H. R. Tan, J. P. Y. Tan, S. C. Ng, E. Teo,*Cryst. Growth Des*., 2012, **12**, 3296.

31 V. Privman, D. V. Goia, J. Park, E. Matijević, *J. Colloid Interf. Sci.*, 1999, **213**, 36.

32 P. Georgiou, K. Kolokotronis, J. Simitzis, *J. Nanopart. Res.*, 2009, **6**, 157.

33 M. Sudha, S. Senthilkumar, R. Hariharan, A. Suganthi, M. Rajarajan, *J. Sol-Gel Sci. Technol.*, 2013, **65**, 301.

34 C. -L. Zhang, S.-H. Yu, *Chem. Soc. Rev.,* 2014, **43**, 4423.

35 P. A. McCarthy, J. Huang, S. -C. Yang, H. -L. Wang, *Langmuir*, 2002, **18**, 259.

36 H. Hu, J. L. Cadenas, J. M. Saniger, P. K. Nair, *Polym. Int.*, 1998, **45**, 262.

37 A. Wei, L. Pan, W. Huang, *Mater. Sci. Eng. B*, 2011, **176**, 1409.

38 J. R. Anusha, H. -J. Kim, A. T. Fleming, S. J. Das, K. -H. Yu, B. C. Kim, C. J. Raj, *Sens. Actuators B*, 2014, **202**, 827.

39 J. Wang, in *Analytical Electrochemistry*, ed. A John Wiley & Sons Inc., New York, 2nd edn., 2000, ch. 2, pp. 28-59.

40 B. C. Janegitz, F. A. dos Santos, R. C. Faria, V. Zucolotto, *Mat. Sci. Eng. C*, 2014, **37**, 14.

41 J. Ding, S. Zhu, T. Zhu, W. Sun, Q. Li, G. Wei, Z. Su, RSC Adv., 2015, **5**, 22935-22942.

42 Y. Li, J. Li, X. H. Xia, S. Liu, Talanta, 2010, **82**, 1164-1169.

43 Y. Ni, J. Zhu, L. Zhang, J. Hong, CrystEngComm, 2010, **12**, 2213–2218.

44 X. Zhang, W. Ma, H. Nan, G. Wang, Electrochim. Acta, 2014,**144**, 186–193.

Improving the electrochemical properties of polyamide 6/polyaniline electrospun nanofibers by surface modification with ZnO nanoparticles.

Rafaela S. Andre,[1,2] Adriana Pavinatto,[1] Luiza A. Mercante,[1] Elaine C. Paris,[1,2] Luiz H. C. Mattoso,[1,2] Daniel S. Correa[1,2]*

Graphic Abstract

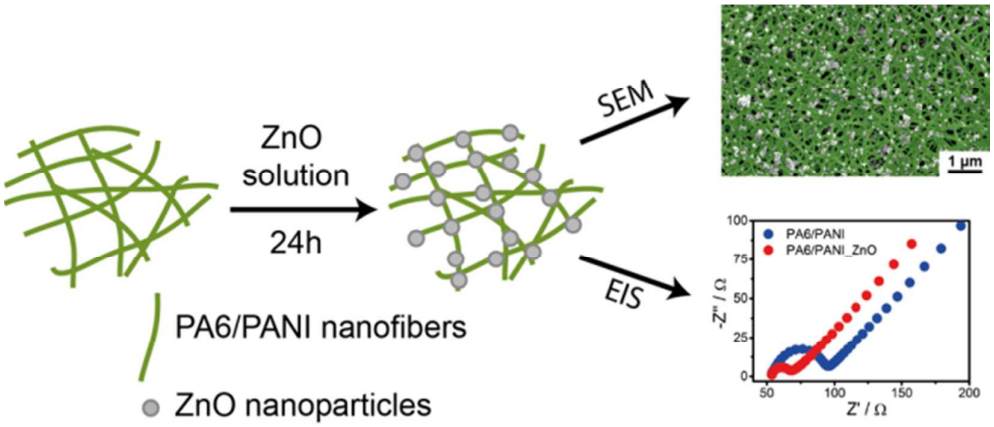

ZnO nanoparticles adsorbed onto electrospun nanofibers surface improves the electron transfer kinetic and increases the electrode electroactive area. The modified electrodes can be a potential platform for electrochemical applications.

.